

3D modelling of HTS ring magnets

Min Zhang

Department of Electronic and Electrical
Engineering
University of Strathclyde
Glasgow, UK
min.zhang@strath.ac.uk

Muhammad Zulfiqar Ali

Department of Electronic and Electrical
Engineering
University of Strathclyde
Glasgow, UK

Felix Huber

Department of Electronic and Electrical
Engineering
University of Strathclyde
Glasgow, UK

Abstract— We have developed a 3D model for HTS ring shape magnets using homogenised 3D H formulation. Every ten HTS rings are homogenised into one domain in order to speed up the calculation. We have compared the simulation results to experiments performed using field cooling. The model agrees well with experimental results. We then use the model to guide the design of large HTS ring magnets for MRI applications.

Keywords—HTS ring, 3D, H formulation

I. INTRODUCTION (HEADING 1)

A HTS ring magnet is made from YBCO coated conductor¹ (Superpower M4 AP tape with 20 μm copper stabilizer). Each sample conductor is 88 mm in length. Laser cutting was used to cut the tape in the center for 72 mm and each 8mm tape was left intact on both ends as shown in Fig 2(a). Fig 2(b) shows the critical current of one HTS tape after splitting. The critical current of a tape measured by the manufacturer was 520 A at 77 K. After splitting, the critical current reduces to 490 A. 100 of HTS rings are stacked together to form a ring stack. The former inside the HTS ring is 20 mm in diameter. A doublelayered ring stack is used in this experiment as shown in Fig. 1 (a) and (b), by placing two ring stacks together. Due to the asymmetric geometry, the closed side of the magnet sees two HTS layers closely stacked together while the opened side of the magnet sees a 12 mm gap between two HTS layers as shown in Fig. 3a and 3b. This geometry gives a freedom in the selection of the inner diameter of the magnet. In addition, each ring works independently so any local degradation will not degrade the performance of whole magnet. The stacked ring magnet was placed in a brass holder and impregnated with paraffin wax mixed with Aluminium nitride. Fig 1. (c) shows the sample holder after impregnation. The outer diameter of the magnet holder is 90 mm. Three hall sensors are positioned respectively in the centre (H3), 4.5mm from the center towards the closed side (H4) and 4.5 mm from the center towards the opened side (H2), as shown in Fig.1 (d). These sensors are mounted on a double sided PCB board: H2 and H4 are on same side and H3 is on the opposite side.

II. MODELLING

To help understand the physics of HTS ring magnets, a three-dimensional finite element modelling was performed using the homogenised H formulation^{4,3}. The 3D governing equation can be represented by the general form:

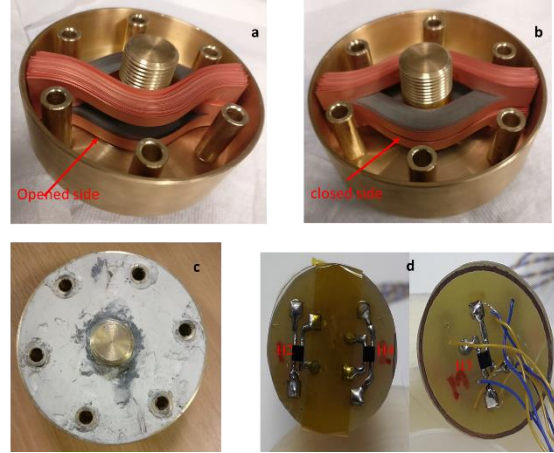


FIG 1. (a) and (b) show the double layered ring magnet sitting in a brass holder. The opened side and the closed side of the ring are indicated respectively. (c) after paraffin impregnation. (d) Hall sensor mounted on double sided PCB board.

$$\mu_0 \mu_r \frac{\partial H}{\partial t} + \nabla \times (\rho \nabla \times H) = 0 \quad (3)$$

where $H = [H_x, H_y, H_z]^T$, $\rho = [\rho_x, \rho_y, \rho_z]^T$ is the resistivity. For HTS domains, ρ is governed by the E-J power law²¹. The magnetic field dependence of critical current density $J_c(B)$ is considered in the model using direct interpolation of measurements of $J_c(B)$ at 25 K.

The HTS ring magnet has 200 rings with a 3D asymmetric geometry, it is not possible to model all the rings in detail due to the high aspect ratio of 2G HTS. The previous established H formulation homogenisation¹⁹ takes two assumptions into account; first the thickness of HTS has been artificially increased from 1 μm to 74 μm , which is the total thickness of the HTS tape; secondly, it is assumed that every ten HTS rings has the same critical current penetration depth. Therefore, every ten HTS rings is homogenised as a single HTS domain, which means the ten HTS rings have the same current distribution. One layer of HTS rings with 100 tapes is therefore represented by ten HTS domains, separated by nine air domains. There is an air domain between each two layers of HTS domains. Fig. 2 shows the comparison between experiment and modelling results. The model employs a much fast ramping current of external magnetic fields due to calculation time limits so Fig. 2 is shown in a normalised time plot. Solid lines are for experiment results and the dotted lines are for the modelling results. The difference between the modelling result and the experimental result is less than 7%.

Fig. 3 illustrates the current distributions in the HTS ring during a FC cycle, corresponding to five different time steps. The current distributions in the rings are not uniform, affecting by the critical current density distribution and the magnetic field distribution. The current is induced simultaneously from the innermost and the outermost HTS domains when the magnetisation starts. When the applied field is further reduced, more current is induced in middle HTS domains and the penetration depth of each HTS domain is increasing.

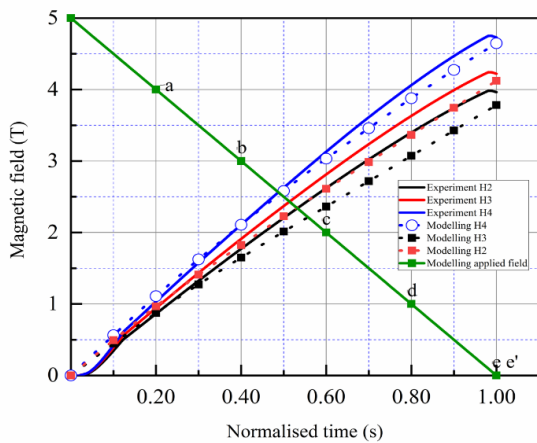


Fig.2. Simulation results. Points a, b, c, d, e and e' show the time steps for normalised current distribution shown in Fig.9. The calculation uses a 10s ramping rate for the magnetic field.

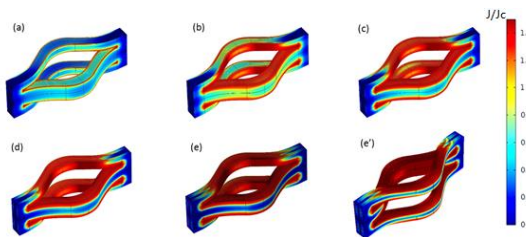


Fig.3. The distribution of the normalised current density (J/J_c) in the ring magnet during the ramping down process. (a) applied field = 4 T, (b) applied field = 3 T, (c) applied field = 2 T, (d) applied field = 1 T, (e) applied field = 0 T for the closed side and (e') applied field = 0 T for the opened side.

Fig.4 shows the current distribution in individual HTS domains and the total current induced in the rings during the field cooling process. Ring 1-10 indicate the innermost domain while ring 91-100 indicate the outermost domain. When the applied field reduced, the inner and outer domains

start to induce persistent current loops to compensate the field reduction from the applied field. The current in the inner and outer domain reaches its peak value at 20% of applied field reduction. This saturation of inner and outer rings' current leads to a weakened shielding effects for the middle domains and forces the current to be induced in the middle rings. This process continues until all the domains saturates. The middle domains with ring 41-60 have the highest current flowing in them after the magnetisation. The changing magnetic field decreases the critical current of the outer and inner rings, so maximum induced current value is also limited by the reduction in critical current. According to Fig.7 (e) and (e'), the outermost domain is not fully penetrated even when the magnetisation is finished. This is because it has the highest critical current density.

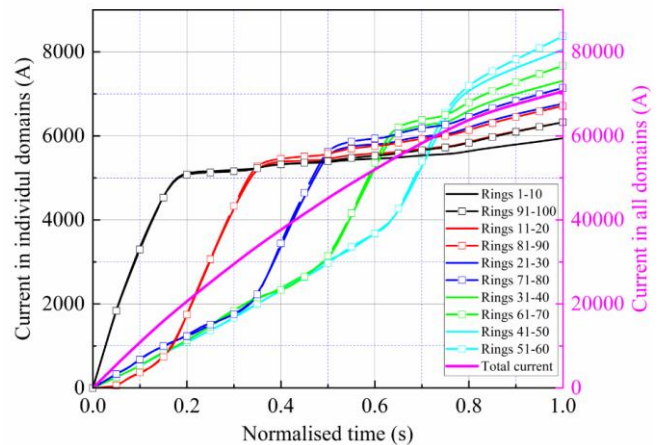


Fig.10. Calculated induced currents in 10 HTS domains during the 5T field cooling process.

REFERENCES

- [1] J. Sheng, M. Zhang, Y. Wang, X. Li, J. Patel, and W. Yuan, *Supercond. Sci. Technol.* 30, 094002 (2017).
- [2] Ruilin Pei, A. Velichko, Zhiyong Hong, Yudong Jiang, Weijia Yuan, A.M. Campbell, and T.A. Coombs, *IEEE Trans. Appl. Supercond.* 19, 3356
- [3] V. S. d. Cruz, G. T. Telles, B. M. O. Santos, A. C. Ferreira and R. De Andrade Junior, "Study of the Voltage Behavior of Jointless Superconducting 2G Loops during Pulse Magnetization," in *IEEE Transactions on Applied Superconductivity*.
- [4] Z. Hong, A.M. Campbell, and T.A. Coombs, *Supercond. Sci. Technol.* 19, 1246 (2006). I. S. Jacobs and C. P. Bean, "Fine particles, thin films and exchange anisotropy," in *Magnetism*, vol. III, G. T. Rado and H. Suhl, Eds. New York: Academic, 1963, pp. 271–350.